

The Age of Olfactory Bulb Neurons in Humans

Olaf Bergmann,¹ Jakob Liebl,⁴ Samuel Bernard,⁵ Kanar Alkass,² Maggie S.Y. Yeung,¹ Peter Steier,⁴ Walter Kutschera,⁴ Lars Johnson,³ Mikael Landén,^{3,6} Henrik Druid,² Kirsty L. Spalding,^{1,*} and Jonas Frisén^{1,*}

¹Department of Cell and Molecular Biology

²Department of Oncology-Pathology

³Division of Psychiatry, Department of Clinical Neuroscience
Karolinska Institute, SE-17177 Stockholm, Sweden

⁴University of Vienna, Faculty of Physics – Isotope Research, AT-1090 Vienna, Austria

⁵Institut Camille Jordan, CNRS UMR 5208, University of Lyon, FR-69622 Villeurbanne, France

⁶Institute of Neuroscience and Physiology, Sahlgrenska Academy at Gothenburg University, SE-40530 Gothenburg, Sweden

*Correspondence: kirsty.spalding@ki.se (K.L.S.), jonas.frisen@ki.se (J.F.)

DOI 10.1016/j.neuron.2012.03.030

SUMMARY

Continuous turnover of neurons in the olfactory bulb is implicated in several key aspects of olfaction. There is a dramatic decline postnatally in the number of migratory neuroblasts en route to the olfactory bulb in humans, and it has been unclear to what extent the small number of neuroblasts at later stages contributes new neurons to the olfactory bulb. We have assessed the age of olfactory bulb neurons in humans by measuring the levels of nuclear bomb test-derived ¹⁴C in genomic DNA. We report that ¹⁴C concentrations correspond to the atmospheric levels at the time of birth of the individuals, establishing that there is very limited, if any, postnatal neurogenesis in the human olfactory bulb. This identifies a fundamental difference in the plasticity of the human brain compared to other mammals.

INTRODUCTION

Neural stem cells residing in the walls of the lateral ventricles of the brain give rise to neuroblasts that migrate to the olfactory bulb throughout life (Lois et al., 1996; Ming and Song, 2011). The new neurons integrate into the synaptic circuitry and are implicated in complex processes such as olfactory memory formation, odorant discrimination, and social interactions (Carlén et al., 2002; Lazarini and Lledo, 2011). Olfactory bulb neurogenesis is well characterized in rodents and has been shown to persist in adult monkeys (Kornack and Rakic, 2001), but the extent and potential role of postnatal olfactory bulb neurogenesis in humans is unclear. Anosmia is a common and early symptom in neurodegenerative diseases such as Alzheimer's and Parkinson's disease, and it has been suggested that this may be due to reduced adult olfactory bulb neurogenesis (Höglinger et al., 2004; Winner et al., 2011).

There are neural stem cells lining the lateral ventricles in the adult human brain (Johansson et al., 1999; Sanai et al., 2004), but it was controversial to what extent they give rise to neuroblasts that migrate to the olfactory bulb (Curtis et al., 2007; Sanai

et al., 2004). Recently, two studies demonstrated a dramatic decline in the number of cells with a marker profile and morphology of migratory neuroblasts after birth in humans (Sanai et al., 2011; Wang et al., 2011). However, both studies found neuroblasts also in adult subjects, albeit the cells did not form a distinct migratory stream but appeared as individual cells and at a very much lower frequency than in the perinatal period (Sanai et al., 2011; Wang et al., 2011).

It is difficult to infer the extent of neurogenesis from the number of neuroblasts, as it is not possible to know whether the neuroblasts differentiate to mature neurons and integrate stably in the circuitry. Even in a situation in which a very small number of neuroblasts are present at any given time, the neuroblasts could potentially give rise to a substantial proportion of olfactory bulb neurons if they would integrate efficiently and if this process would be continuous over a long time. Moreover, there are also neural stem cells present in the adult rodent and human olfactory bulb, and new neurons may not only derive from the ventricle wall but may be generated locally in the olfactory bulb (Gritti et al., 2002; Pagano et al., 2000).

Due to the important role of adult olfactory bulb neurogenesis in experimental animals and the suggested alteration of this process underlying common symptoms of neurodegenerative diseases, we set out to establish to what extent this process is operational in humans. We report that there is a continuous turnover of nonneuronal cells throughout life but that there is minimal, if any, addition of new neurons after the perinatal period in humans.

RESULTS AND DISCUSSION

Cell Turnover in the Human Olfactory Bulb

We have determined the age of olfactory bulb cells by measuring the concentration of nuclear bomb test-derived ¹⁴C in genomic DNA (Spalding et al., 2005a). Atmospheric ¹⁴C levels were stable until nuclear bomb tests conducted during the Cold War resulted in a dramatic increase (De Vries, 1958; Nydal and Lövseth, 1965). There have been no major above ground nuclear tests after the International Test Ban Treaty in 1963, and the atmospheric ¹⁴C levels have since declined due to uptake by the biotope and diffusion from the atmosphere (Levin and Kromer, 2004; Levin et al., 2010). ¹⁴C in the atmosphere reacts with oxygen to form

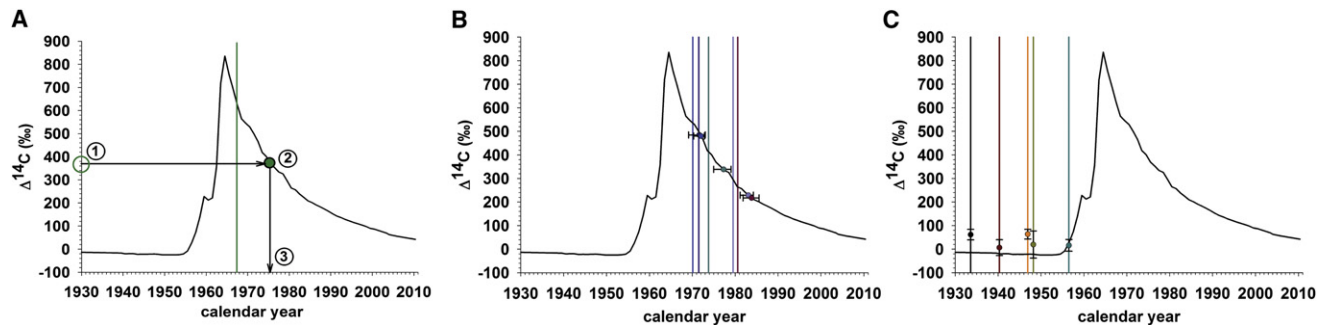


Figure 1. Postnatal Cell Turnover in the Human Olfactory Bulb

(A) Schematic illustration of the strategy to establish cell age by ^{14}C dating. The black curve shows the excess of the atmospheric ^{14}C concentrations over the natural level ($\Delta^{14}\text{C} = 0$) (data from Levin and Kromer, 2004; Levin et al., 2010), and the vertical line indicates the date of birth of the studied individual in all figures. The measured genomic ^{14}C concentration (1) is related to the atmospheric ^{14}C concentration at or after the person was born (2). The birth date of a cell population is then read off the x axis (3). (B and C) The ^{14}C concentration in genomic DNA from human olfactory bulb cells in subjects born after (B) or before (C) the nuclear bomb tests corresponds to time points after the time of birth, demonstrating postnatal cell turnover. A vertical line and a dot of the same color indicate the date of birth and ^{14}C data, respectively, for each individual. Error bars for subjects born after the nuclear bomb tests are given in years by calibrating to atmospheric ^{14}C concentrations (see Supplemental Experimental Procedures). Analysis of individuals born before the increase in the atmospheric ^{14}C concentration provides high sensitivity to detect whether any cell renewal occurs later in life, but it is not possible to directly infer the age of the cell population, and therefore the error bars indicate the measurement error in ^{14}C concentration in the respective DNA sample.

$^{14}\text{CO}_2$ and enters the food chain through plant photosynthesis. By eating plants and animals that live off plants, the ^{14}C concentration in the human body closely parallels that in the atmosphere at any given time (Harkness, 1972; Libby et al., 1964; Spalding et al., 2005b). When cells undergo mitosis and duplicate their DNA, they integrate ^{14}C with a concentration corresponding to that in the atmosphere, resulting in a stable date mark. By measuring ^{14}C in genomic DNA and determining when the corresponding ^{14}C concentration was present in the atmosphere, it is possible to establish the birth date of cells (Figure 1A) and their turnover dynamics (Bergmann et al., 2009; Bhardwaj et al., 2006; Spalding et al., 2005a, 2008). Changes in DNA methylation can alter the ^{14}C content of DNA, but not to a degree that can influence the analysis of cell turnover (Spalding et al., 2005a). ^{14}C abundance can be measured by accelerator mass spectrometry, and we developed a protocol to enable analysis with increased sensitivity (see Supplemental Experimental Procedures available online).

Analysis of the ^{14}C concentration in postmortem olfactory bulb genomic DNA from adult humans revealed levels corresponding to time points after the birth of the individual, establishing that there is significant postnatal cell turnover in the human olfactory bulb ($p < 0.02$; Figures 1B and 1C; Table S1 and Supplemental Information). The oldest studied individual, born more than 20 years before the onset of the increase in atmospheric ^{14}C levels, had a ^{14}C concentration significantly higher than that present in the period up to 1955, establishing that there is substantial cell turnover at least up to early adulthood in humans (Figure 1C). However, several of the individuals born before 1950 had genomic ^{14}C concentrations lower than at any time after the onset of the nuclear bomb tests, indicating that there must be very long-lived cells in the olfactory bulb that have remained for more than 50 years. The human olfactory bulb contains approximately equal numbers of neurons and nonneuronal cells, and it is not possible to conclude from this data whether all cell

types are exchanged or if cell turnover is restricted to one of these populations.

Isolation of Neuronal and Nonneuronal Nuclei

In order to specifically establish the age and turnover of neurons and nonneuronal cells, respectively, we isolated neuronal nuclei labeled with an antibody to NeuN (Fox3) by flow cytometry (Figures 2A and 2B) (Bhardwaj et al., 2006; Spalding et al., 2005a). NeuN has been extensively validated as a marker for most neuronal subsets, but mitral cells and some glomerular layer neurons in the olfactory bulb are not immunoreactive to NeuN in rodents (Mullen et al., 1992). Histological analysis revealed that there is a small subset of neurons also in the human olfactory bulb that are NeuN $^-$ (Figure 2C). We therefore wanted to develop an additional strategy to isolate neuronal nuclei from the human olfactory bulb, which would not exclude any neuronal subtype. We used antibodies to the RNA binding protein HuD, which is specific to postmitotic neurons (Barami et al., 1995), to isolate nuclei from the adult human olfactory bulb (Figures 2D and 2E). Histological analysis confirmed that HuD antibodies label all cells with neuronal characteristics in the adult human olfactory bulb (Figure 2F and Figure S1). However, we found that HuD antibodies, in addition to neurons, also labeled a subset of nonneuronal cells (Figure 2F). Histology and flow cytometry revealed that the nonneuronal population labeled with HuD antibodies had oligodendrocyte morphology and coexpressed the oligodendrocyte lineage markers Sox10 and CNPase (Figures 2E and 2F and Figures S2 and S3). Thus, by isolating cell nuclei that were HuD+ and Sox10 $^-$, we were able to specifically isolate neuronal nuclei (Figure 2E). All NeuN+ nuclei were within the HuD+/Sox10 $^-$ population and $93.5\% \pm 3.6\%$ (mean \pm SD) of HuD+/Sox10 $^-$ nuclei were NeuN+, in line with only a small subpopulation of neurons being NeuN $^-$ in the adult human olfactory bulb. We used both these isolation strategies to birth date neurons and nonneuronal cells.

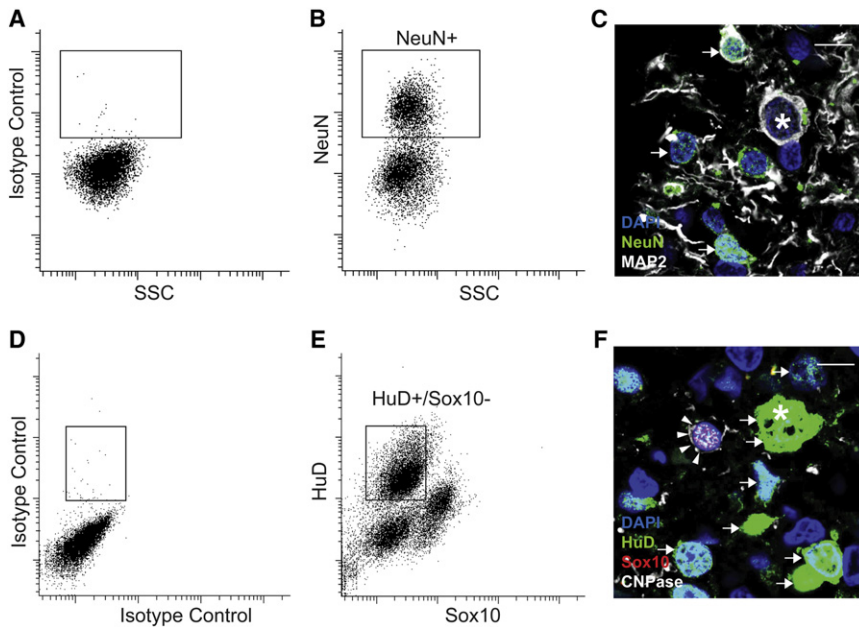


Figure 2. Identification and Isolation of Neuronal Nuclei in the Human Olfactory Bulb

(A and B) Nuclei were labeled with isotype control antibody (A) or with antibodies to NeuN/Fox3 (B). (C) Antibodies to NeuN label most neurons (arrows), but not large neurons in the mitral/granular layer. (D and E) Nuclei were labeled with isotype control antibody (D) and neuronal nuclei were identified by the presence of HuD and the absence of Sox10 (E). (F) HuD antibodies label mitral cells (asterisk), other neurons (arrows), and a subset of oligodendrocyte lineage cells identified by Sox10 and CNPase expression (arrowheads). Arrows indicate NeuN+ (C) or HuD+/Sox10- (E) neuronal nuclei. The sorting gates for neuronal nuclei are indicated in (B) and (E). SSC, side scatter. Scale bars indicate 10 μ m.

New Nonneuronal Cells in the Adult Human Olfactory Bulb

Analysis of the ^{14}C concentration in genomic DNA from isolated nonneuronal nuclei from the adult human olfactory bulb revealed levels corresponding to concentrations well after the birth of the individual in all cases, establishing substantial turnover of nonneuronal cells ($p = 0.0002$; Figure 3; see Supplemental Information). Integrating data from several individuals born at different times in relation to the nuclear bomb tests allows estimating the turnover dynamics of a cell population (Bergmann et al., 2009; Spalding et al., 2008). This indicated an annual turnover rate of 2.0%–3.4% in the nonneuronal cell population (see Supplemental Information). This represents an average for all cells negative for the respective neuronal marker profile, and it is likely that the turnover dynamics vary between specific nonneuronal cell types.

Olfactory Bulb Neurons Are as Old as the Person

We next assessed the ^{14}C concentration in genomic DNA from NeuN+ or HuD+/Sox10- neuronal nuclei. In all cases ($n = 15$), the ^{14}C concentration in neuronal genomic DNA was very close to that present in the atmosphere at the time of birth of each individual (Figure 4) and not significantly different from what one would see if there was no postnatal generation of olfactory bulb neurons ($p = 0.91$; see Supplemental Information). We cannot exclude that there may be low-grade turnover of neurons, but at a constant rate, the annual turnover would be $0.008\% \pm 0.08\%$ (mean \pm SE; see Supplemental Information). That corresponds to <1% of neurons being exchanged after 100 years. It has been estimated that up to 50% of olfactory bulb neurons are exchanged annually in rodents (Imayoshi et al., 2008), and if there is any postnatal olfactory bulb neurogenesis in humans, its extent is orders of magnitude lower.

Neurodegenerative and psychiatric diseases and substance abuse have been suggested to reduce olfactory bulb neurogen-

esis (Hansson et al., 2010; Höglinger et al., 2004; Negoias et al., 2010; Turetsky et al., 2000; Winner et al., 2011). Some individuals in our study were diagnosed with one or more of these conditions (Table S2). However, as all studied individuals had neuronal ^{14}C concentrations corresponding to the time around birth, we did not find any apparent correlation between these conditions and postnatal olfactory bulb neurogenesis in humans. Anosmia is a common and early symptom in several neurodegenerative diseases, and it has been suggested to be related to reduced adult olfactory bulb neurogenesis (Höglinger et al., 2004; Winner et al., 2011), but this appears unlikely.

Functional studies in rodents have implicated adult neurogenesis in olfactory memory formation, odorant discrimination, and social interactions (Lazarini and Lledo, 2011). The lack of comparable adult olfactory bulb neurogenesis in humans poses the question whether these functions are mediated by conceptually different mechanisms in humans, or whether the more limited dependence on olfaction in humans compared to rodents in part may be due to the lack of one type of plasticity, adult neurogenesis.

EXPERIMENTAL PROCEDURES

Tissue Collection

Tissues were procured from cases admitted during 2005 and 2011 to the Department of Forensic Medicine in Stockholm for autopsy, after informed consent from relatives. Ethical permission for this study was granted by the Regional Ethical Committee in Stockholm. Whole olfactory bulbs from both hemispheres were analyzed. Cerebellar cortex samples from the same subjects served as controls. Brain tissue was frozen and stored at -80°C until further analysis.

Nuclei Isolation

Tissue samples were thawed and Dounce homogenized in 10 ml lysis buffer (0.32 M sucrose, 5 mM CaCl_2 , 3 mM magnesium acetate, 0.1 mM EDTA, 10 mM Tris-HCl [pH 8.0], 0.1% Triton X-100, and 1 mM DTT). Homogenized samples were suspended in 20 ml of sucrose solution (1.7 M sucrose, 3 mM magnesium acetate, 1 mM DTT, and 10 mM Tris-HCl [pH 8.0]), layered onto a cushion of 10 ml sucrose solution, and centrifuged at $36,500 \times g$ for 2.4 hr

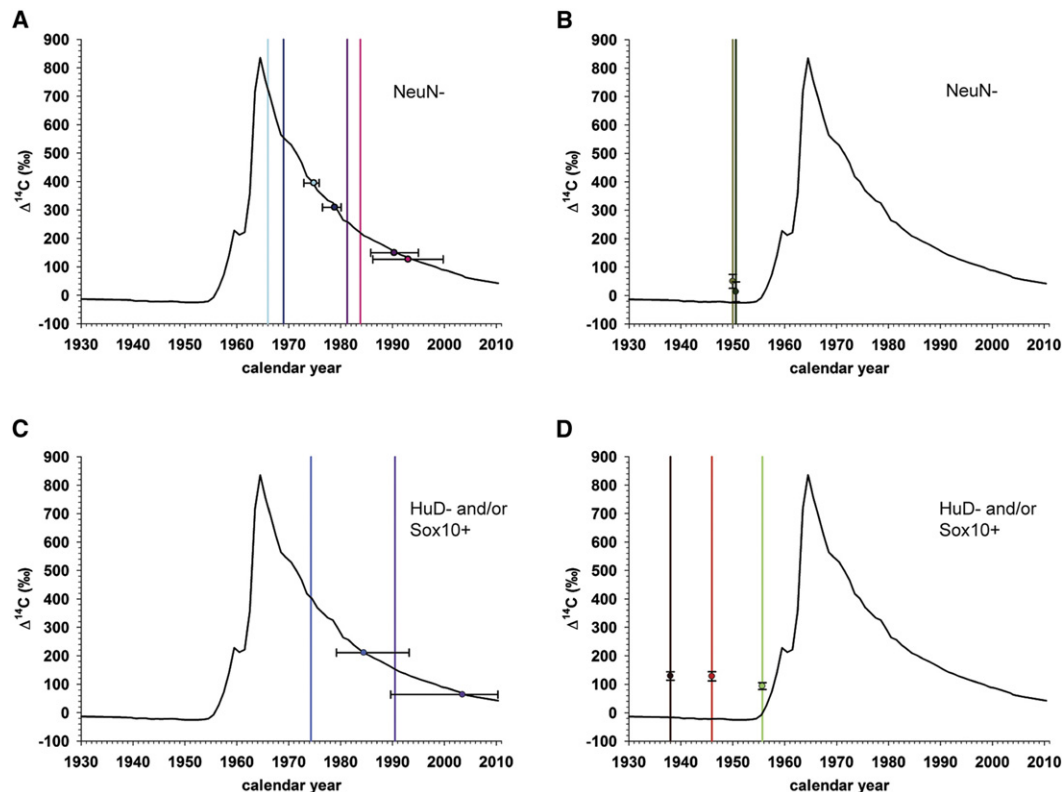


Figure 3. Turnover of Nonneuronal Cells

The ^{14}C concentration in genomic DNA from nonneuronal cells, defined by the absence of NeuN labeling (A and B) or not being HuD+/Sox10– (C and D), corresponds to time points well after the birth of each individual. The vertical bar indicates the year of birth of the individual, with the correspondingly colored data point indicating the ^{14}C concentration. Error bars indicate two standard deviations in ^{14}C concentration in the respective DNA sample.

at 4°C . The isolated nuclei were resuspended in nuclei storage buffer (NSB) (10 mM Tris [pH 7.2], 2 mM MgCl_2 , 70 mM KCl, and 15% sucrose) for consecutive immunostaining and flow cytometry analysis.

FACS Sorting and Analysis

Isolated nuclei were stained with mouse NeuN (A-60) (Millipore, 1:1,000), rabbit Fox3 (Atlas Antibody, 1:300), mouse HuD (E-1) (Santa Cruz, 1:100), mouse HuD/HuC 16A11-biotin (Invitrogen, 1:300), or goat Sox10 (R&D, 1:300). NeuN (A-60) antibody was directly conjugated to Alexa 647 (Invitrogen Antibody Labeling Kit Alexa 647). All other primary antibodies were visualized with appropriate secondary antibodies conjugated to Alexa 488 (1:500), Alexa 647 (1:500) (Invitrogen), or R-phycoerythrin (PE) (Santa Cruz, 1:100). Flow cytometry sorting was performed with a BD FACS Diva and flow cytometry analysis was performed with a BD FACS Aria instrument.

Immunohistochemistry

Olfactory bulbs were fixed in 4% formaldehyde buffered in PBS for 24 hr and embedded in low-melting paraffin (52°C – 54°C), according to standard procedures. Olfactory bulbs were sectioned ($5\ \mu\text{m}$) longitudinally and orthogonally according to their long axis. For immunohistochemistry, sections were deparaffinized in xylene and rehydrated in a descending ethanol series. Antigen retrieval was performed in citraconic acid solution (pH = 7.4; 0.05% citraconic acid) for 20 min in a domestic steamer (Namimatsu et al., 2005). The sections were allowed to cool down for 20 min before immunostaining was started. Sections were incubated with the respective primary antibody overnight at 4°C : mouse NeuN (Millipore A-60 clone; 1:100), rabbit Fox3 (Atlas Antibody, 1:300), goat Sox10 (R&D, 1:100), rabbit calbindin (Abcam, 1:200), chicken MAP-2 (Abcam, 1:1,000), rabbit calretinin (Abcam, 1:200), rabbit parvalbumin

(Abcam, 1:1,000), rabbit tyrosine hydroxylase (TH) (Millipore, 1:1,000), rabbit GAD65/67 (Millipore, 1:500), rabbit CNPase (Atlas Antibody, 1:400), mouse GFAP (Sigma Aldrich, 1:1,000), rabbit Iba1 (Wako, 1:1,000), mouse HuD (E-1) (Santa Cruz, 1:100), and mouse HuD/HuC 16A11-biotin (Invitrogen, 1:100), and visualized with the matching secondary antibody and streptavidin conjugated to Alexa 488, 546, or 647 (1:1,000, Invitrogen).

DNA Purification

All experiments were carried out in a clean room (ISO8) to prevent any carbon contamination of the samples. All glassware was prebaked at 450°C for 4 hr. DNA isolation was performed according to a modified protocol from Miller et al. (1988). Five hundred microliters of DNA lysis buffer (100 mM Tris [pH 8.0], 200 mM NaCl, 1% SDS, and 5 mM EDTA) and $6\ \mu\text{l}$ Proteinase K (20 mg/ml) were added to the collected nuclei and incubated overnight at 65°C . RNase cocktail (Ambion) was added and incubated at 65°C for 1 hr. Half of the existing volume of 5 M NaCl solution was added and agitated for 15 s. The solution was spun down at 13,000 rpm for 3 min. The supernatant containing the DNA was transferred to a 12 ml glass vial. Three times the volume of absolute ethanol was added, and the glass vial was inverted several times to precipitate the DNA. The DNA precipitate was washed three times in DNA washing solution (70% Ethanol [v/v] and 0.5 M NaCl) and transferred to $500\ \mu\text{l}$ DNase/RNase free water (GIBCO/Invitrogen). The DNA was quantified and DNA purity verified by UV spectroscopy (NanoDrop).

Accelerator Mass Spectrometry

^{14}C accelerator mass spectrometry (AMS) measurements were performed on graphitized samples. DNA in aqueous solution was freeze dried, combusted to CO_2 , and reduced to graphite according to the procedures described in

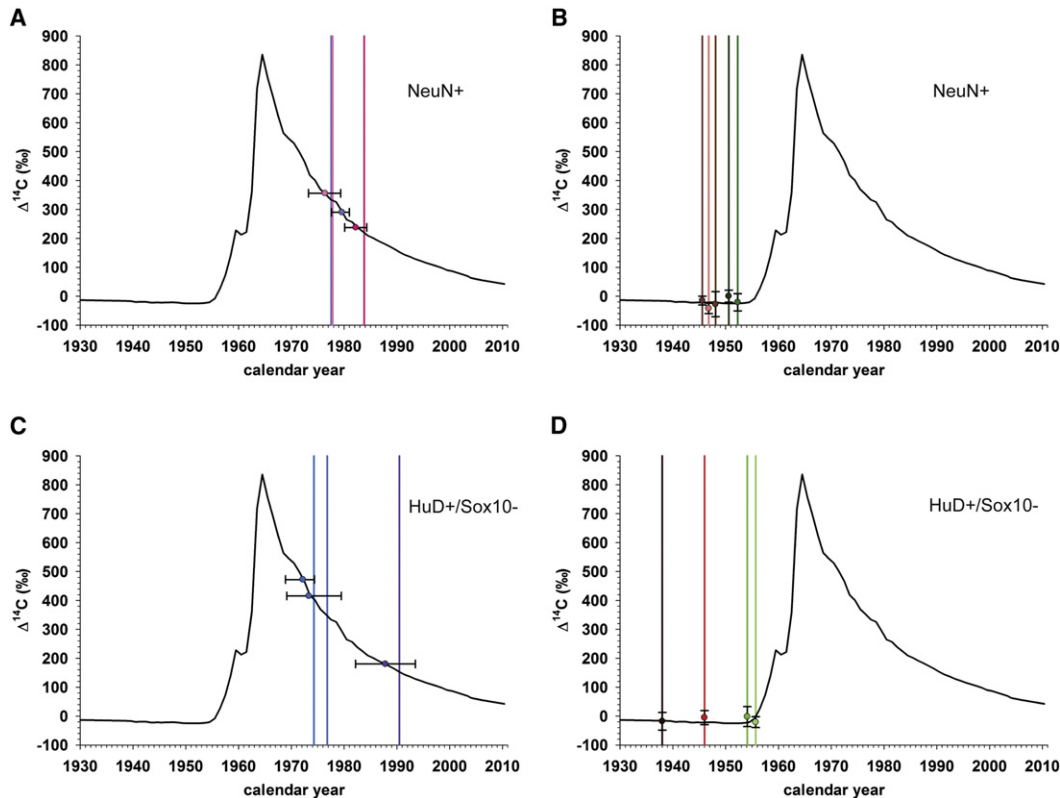


Figure 4. Limited Neurogenesis in the Adult Human Olfactory Bulb

^{14}C concentrations in genomic DNA from neuronal nuclei isolated with antibodies against NeuN (A and B) or by the marker combination HuD+/Sox10– (C and D) were not significantly different from atmospheric ^{14}C concentrations at birth. The vertical bars indicate the year of birth of each individual, with the correspondingly colored data point indicating the ^{14}C concentration. Error bars indicate two standard deviations in ^{14}C concentration in the respective DNA sample.

Liebl et al. (2010). ^{14}C AMS measurements of graphitized samples were carried out at the Vienna Environmental Research Accelerator (VERA) of the University of Vienna, a 3 MV Pelletron tandem AMS system (Priller et al., 1997; Rom et al., 1998; Steier et al., 2004). The setup of VERA for heavy isotopes was described earlier (Vockenhuber et al., 2003). ^{14}C measurement results are reported as $F^{14}\text{C}$ according to the recommendation of Reimer et al. (2004). Age calibration of ^{14}C concentrations was performed using the software CALIBomb (<http://calib.qub.ac.uk/CALIBomb>) with the following parameters: smoothing in years, 1 year; resolution, 0.2; ^{14}C calibration, two sigma.

For details related to accelerator mass spectrometry measurements and correction for FACS impurities, see Supplemental Experimental Procedures and Figure S4.

SUPPLEMENTAL INFORMATION

Supplemental Information includes six figures, Supplemental Experimental Procedures, and four tables and can be found with this article online at [doi:10.1016/j.neuron.2012.03.030](https://doi.org/10.1016/j.neuron.2012.03.030).

ACKNOWLEDGMENTS

We thank Marcelo Toro, Albert Busch, and Haythem H.M. Ismail for flow cytometry, Marie-Louise Spångberg for histology, Martina Wennberg and Anna Speles for administrative assistance, and Klaus Mair for preparing carbon samples. This study was supported by the Swedish Research Council, Tobias Stiftelsen, Hjärnfonden, SSF, NARSAD, Knut och Alice Wallenbergs Stiftelse, AFA Försäkringar, the ERC, and the regional agreement on medical training and clinical research between Stockholm County Council and the

Karolinska Institutet (ALF 20080508). J.L. was supported by a research grant of the University of Vienna and O.B. by Deutsche Forschungsgemeinschaft.

Accepted: March 7, 2012

Published: May 23, 2012

REFERENCES

- Barami, K., Iversen, K., Furneaux, H., and Goldman, S.A. (1995). Hu protein as an early marker of neuronal phenotypic differentiation by subependymal zone cells of the adult songbird forebrain. *J. Neurobiol.* 28, 82–101.
- Bergmann, O., Bhardwaj, R.D., Bernard, S., Zdunek, S., Barnabé-Heider, F., Walsh, S., Zupicich, J., Alkass, K., Buchholz, B.A., Druid, H., et al. (2009). Evidence for cardiomyocyte renewal in humans. *Science* 324, 98–102.
- Bhardwaj, R.D., Curtis, M.A., Spalding, K.L., Buchholz, B.A., Fink, D., Björk-Eriksson, T., Nordborg, C., Gage, F.H., Druid, H., Eriksson, P.S., and Frisén, J. (2006). Neocortical neurogenesis in humans is restricted to development. *Proc. Natl. Acad. Sci. USA* 103, 12564–12568.
- Carlén, M., Cassidy, R.M., Brismar, H., Smith, G.A., Enquist, L.W., and Frisén, J. (2002). Functional integration of adult-born neurons. *Curr. Biol.* 12, 606–609.
- Curtis, M.A., Kam, M., Nannmark, U., Anderson, M.F., Axell, M.Z., Wikkelso, C., Holtås, S., van Roon-Mom, W.M., Björk-Eriksson, T., Nordborg, C., et al. (2007). Human neuroblasts migrate to the olfactory bulb via a lateral ventricular extension. *Science* 315, 1243–1249.
- De Vries, H. (1958). Atomic bomb effect: variation of radiocarbon in plants, shells, and snails in the past 4 years. *Science* 128, 250–251.

- Gritti, A., Bonfanti, L., Doetsch, F., Caille, I., Alvarez-Buylla, A., Lim, D.A., Galli, R., Verdugo, J.M., Herrera, D.G., and Vescovi, A.L. (2002). Multipotent neural stem cells reside into the rostral extension and olfactory bulb of adult rodents. *J. Neurosci.* *22*, 437–445.
- Hansson, A.C., Nixon, K., Rimondini, R., Damadzic, R., Sommer, W.H., Eskay, R., Crews, F.T., and Heilig, M. (2010). Long-term suppression of forebrain neurogenesis and loss of neuronal progenitor cells following prolonged alcohol dependence in rats. *Int. J. Neuropsychopharmacol.* *13*, 583–593.
- Harkness, D.D. (1972). Further investigations of the transfer of bomb ^{14}C to man. *Nature* *240*, 302–303.
- Höglinger, G.U., Rizk, P., Muriel, M.P., Duyckaerts, C., Oertel, W.H., Caille, I., and Hirsch, E.C. (2004). Dopamine depletion impairs precursor cell proliferation in Parkinson disease. *Nat. Neurosci.* *7*, 726–735.
- Imayoshi, I., Sakamoto, M., Ohtsuka, T., Takao, K., Miyakawa, T., Yamaguchi, M., Mori, K., Ikeda, T., Itoharu, S., and Kageyama, R. (2008). Roles of continuous neurogenesis in the structural and functional integrity of the adult forebrain. *Nat. Neurosci.* *11*, 1153–1161.
- Johansson, C.B., Svensson, M., Wallstedt, L., Janson, A.M., and Frisén, J. (1999). Neural stem cells in the adult human brain. *Exp. Cell Res.* *253*, 733–736.
- Kornack, D.R., and Rakic, P. (2001). The generation, migration, and differentiation of olfactory neurons in the adult primate brain. *Proc. Natl. Acad. Sci. USA* *98*, 4752–4757.
- Lazarini, F., and Lledo, P.M. (2011). Is adult neurogenesis essential for olfaction? *Trends Neurosci.* *34*, 20–30.
- Levin, I., and Kromer, B. (2004). The tropospheric $^{14}\text{CO}_2$ level in mid latitudes of the northern hemisphere (1959–2003). *Radiocarbon* *46*, 1261–1272.
- Levin, I., Naegler, T., Kromer, B., Diehl, M., Francey, R.J., Gomez-Pelaez, A.J., Steele, L.P., Wagenbach, D., Weller, R., and Worthy, D.E. (2010). Observations and modelling of the global distribution and long-term trend of atmospheric $^{14}\text{CO}_2$. *Tellus* *62*, 26–46.
- Libby, W.F., Berger, R., Mead, J.F., Alexander, G.V., and Ross, J.F. (1964). Replacement Rates for Human Tissue from Atmospheric Radiocarbon. *Science* *146*, 1170–1172.
- Liebl, J., Avalos Ortiz, R., Golser, R., Handle, F., Kutschera, W., Steier, P., and Wild, E.M. (2010). Studies on the preparation of small ^{14}C samples with an RGA and ^{13}C -enriched material. *Radiocarbon* *52*, 1394–1404.
- Lois, C., Garcia-Verdugo, J.-M., and Alvarez-Buylla, A. (1996). Chain migration of neuronal precursors. *Science* *271*, 978–981.
- Miller, S.A., Dykes, D.D., and Polesky, H.F. (1988). A simple salting out procedure for extracting DNA from human nucleated cells. *Nucleic Acids Res.* *16*, 1215.
- Ming, G.L., and Song, H. (2011). Adult neurogenesis in the mammalian brain: significant answers and significant questions. *Neuron* *70*, 687–702.
- Mullen, R.J., Buck, C.R., and Smith, A.M. (1992). NeuN, a neuronal specific nuclear protein in vertebrates. *Development* *116*, 201–211.
- Namimatsu, S., Ghazizadeh, M., and Sugisaki, Y. (2005). Reversing the effects of formalin fixation with citraconic anhydride and heat: a universal antigen retrieval method. *J. Histochem. Cytochem.* *53*, 3–11.
- Negoias, S., Croy, I., Gerber, J., Puschmann, S., Petrowski, K., Joraschky, P., and Hummel, T. (2010). Reduced olfactory bulb volume and olfactory sensitivity in patients with acute major depression. *Neuroscience* *169*, 415–421.
- Nydal, R., and Lövseth, K. (1965). Distribution of radiocarbon from nuclear tests. *Nature* *206*, 1029–1031.
- Pagano, S.F., Impagnatiello, F., Girelli, M., Cova, L., Grioni, E., Onofri, M., Cavallaro, M., Etteri, S., Vitello, F., Giombini, S., et al. (2000). Isolation and characterization of neural stem cells from the adult human olfactory bulb. *Stem Cells* *18*, 295–300.
- Priller, A., Golser, R., Hille, P., Kutschera, W., Rom, W., Steier, P., Wallner, A., and Wild, E.M. (1997). First performance tests of VERA. *Nucl. Instrum. Methods Phys. Res. B* *123*, 193–198.
- Reimer, P.J., Brown, T.A., and Reimer, R.W. (2004). Discussion: reporting and calibration of post-bomb ^{14}C data. *Radiocarbon* *46*, 1299–1304.
- Rom, W., Golser, R., Kutschera, W., Priller, A., Steier, P., and Wild, E.M. (1998). Systematic investigations of ^{14}C measurements at the Vienna Environmental Research Accelerator. *Radiocarbon* *40*, 255–263.
- Sanai, N., Tramontin, A.D., Quiñones-Hinojosa, A., Barbaro, N.M., Gupta, N., Kunwar, S., Lawton, M.T., McDermott, M.W., Parsa, A.T., Manuel-García Verdugo, J., et al. (2004). Unique astrocyte ribbon in adult human brain contains neural stem cells but lacks chain migration. *Nature* *427*, 740–744.
- Sanai, N., Nguyen, T., Ihrle, R.A., Mirzadeh, Z., Tsai, H.H., Wong, M., Gupta, N., Berger, M.S., Huang, E., Garcia-Verdugo, J.M., et al. (2011). Corridors of migrating neurons in the human brain and their decline during infancy. *Nature* *478*, 382–386.
- Spalding, K.L., Bhardwaj, R.D., Buchholz, B.A., Druid, H., and Frisén, J. (2005a). Retrospective birth dating of cells in humans. *Cell* *122*, 133–143.
- Spalding, K.L., Buchholz, B.A., Bergman, L.-E., Druid, H., and Frisén, J. (2005b). Forensics: age written in teeth by nuclear tests. *Nature* *437*, 333–334.
- Spalding, K.L., Arner, E., Westermark, P.O., Bernard, S., Buchholz, B.A., Bergmann, O., Blomqvist, L., Hoffstedt, J., Näslund, E., Britton, T., et al. (2008). Dynamics of fat cell turnover in humans. *Nature* *453*, 783–787.
- Steier, P., Dellinger, F., Kutschera, W., Priller, A., Rom, W., and Wild, E.M. (2004). Pushing the precision limit of ^{14}C AMS. *Radiocarbon* *46*, 5–16.
- Turetsky, B.I., Moberg, P.J., Yousem, D.M., Doty, R.L., Arnold, S.E., and Gur, R.E. (2000). Reduced olfactory bulb volume in patients with schizophrenia. *Am. J. Psychiatry* *157*, 828–830.
- Vockenhuber, C., Ahmad, I., Golser, R., Kutschera, W., Liechenstein, V., Priller, A., Steier, P., and Winkler, S. (2003). Accelerator mass spectrometry of heavy long-lived radionuclides. *Int. J. Mass Spectrom.* *223–224*, 713–732.
- Wang, C., Liu, F., Liu, Y.-Y., Zhao, C.-H., You, Y., Wang, L., Zhang, J., Wei, B., Ma, T., Zhang, Q., et al. (2011). Identification and characterization of neuroblasts in the subventricular zone and rostral migratory stream of the adult human brain. *Cell Res.* *21*, 1534–1550.
- Winner, B., Kohl, Z., and Gage, F.H. (2011). Neurodegenerative disease and adult neurogenesis. *Eur. J. Neurosci.* *33*, 1139–1151.

Neuron, Volume 74

Supplemental Information

The Age of Olfactory Bulb Neurons in Humans

**Olaf Bergmann, Jakob Liebl, Samuel Bernard, Kanar Alkass, Maggie S.Y. Yeung,
Peter Steier, Walter Kutschera, Lars Johnson, Mikael Landén, Henrik Druid, Kirsty L.
Spalding, and Jonas Frisén**

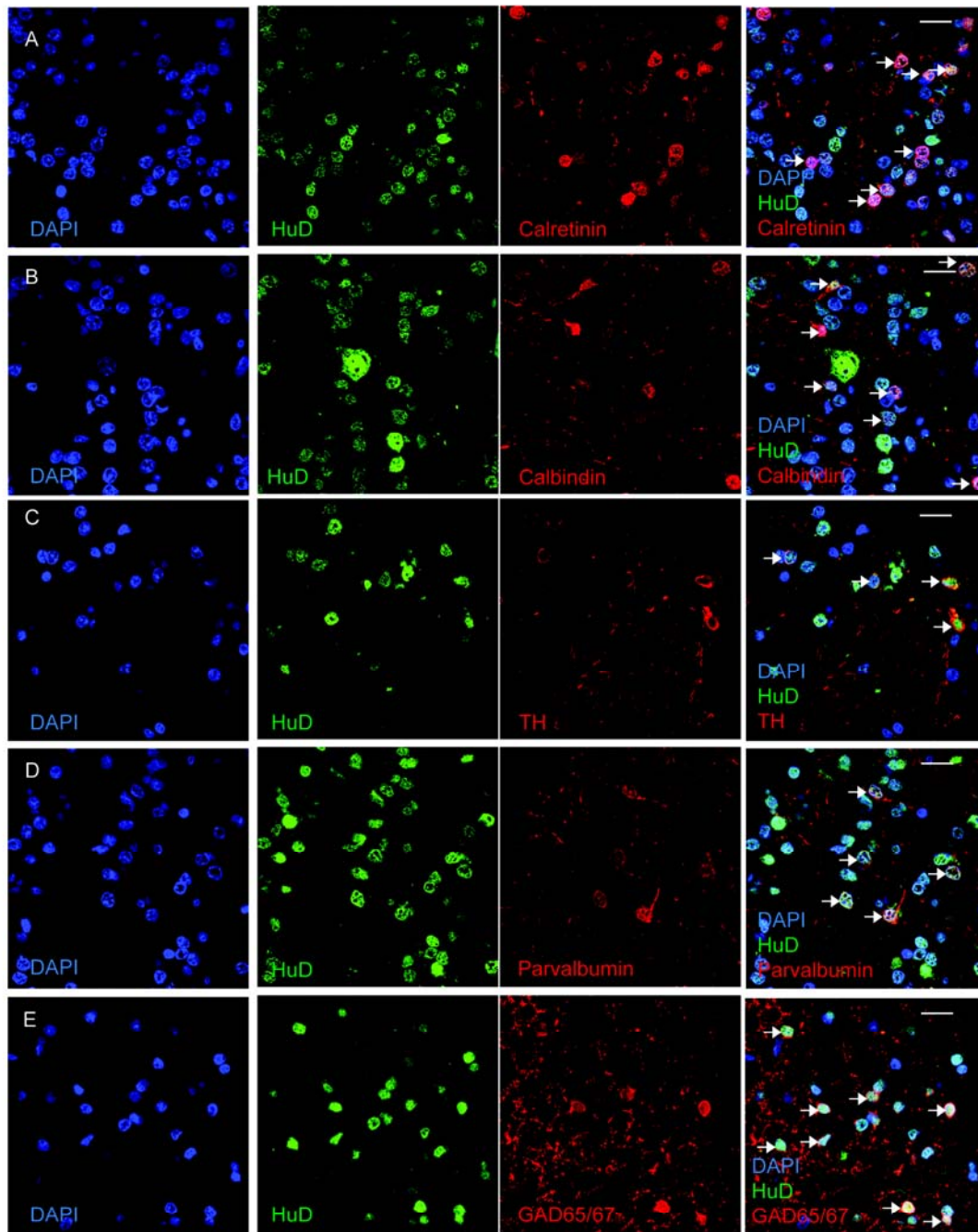


Figure S1, related to Figure 2.

Characterisation of HuD immunoreactivity in the adult human olfactory bulb. HuD expression was visualized by the HuD (E-1) antibody, which had been characterized in the Human Protein Atlas (<http://www.proteinatlas.org>) (Uhlen et al., 2005). HuD (E-1) antibody labels all neuronal subtypes in the human olfactory bulb such as calretinin (A), calbindin (B), tyrosine hydroxylase (TH) (C), parvalbumin (D) and GAD65/67 (E). Scale bars indicate 20 μ m.

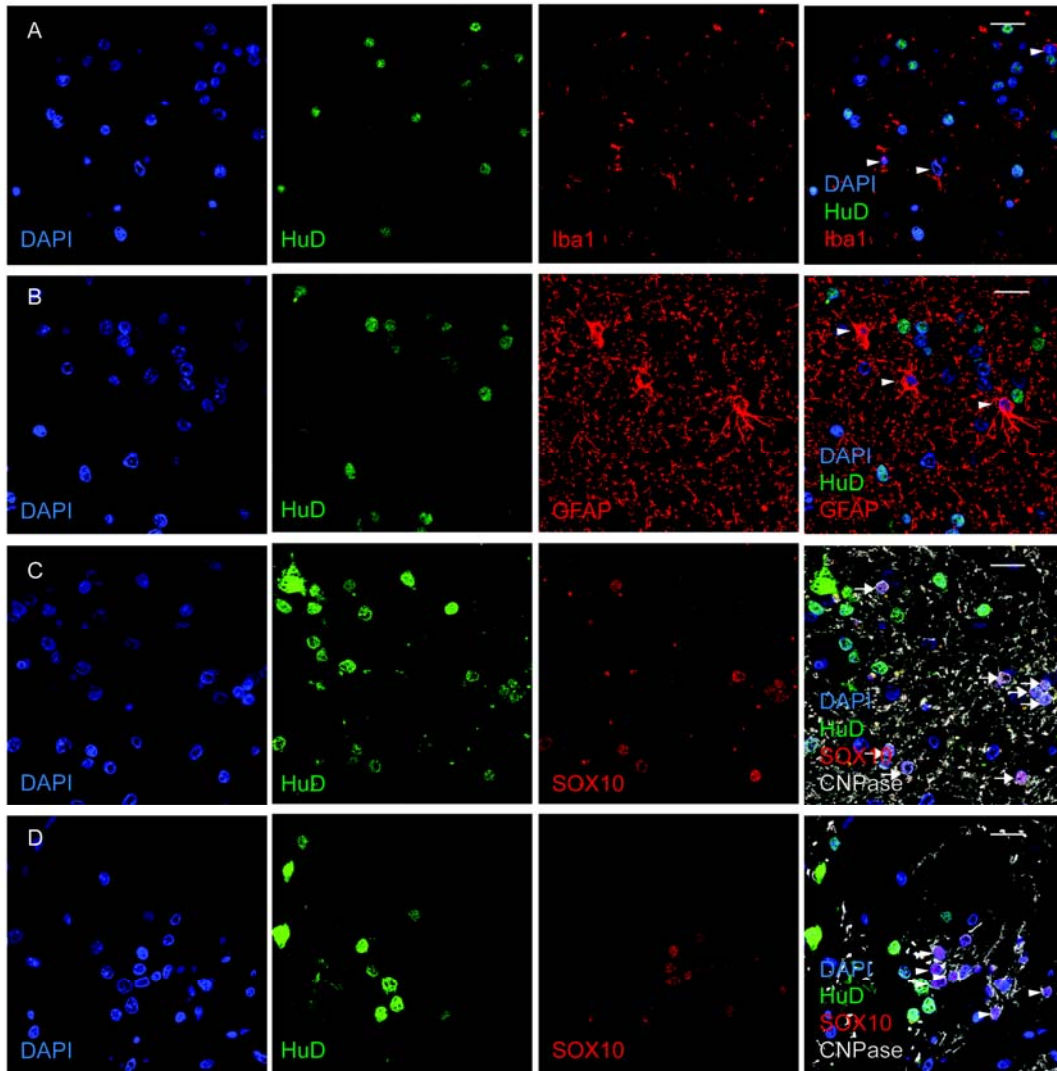


Figure S2, related to Figure 2.

Characterisation of HuD immunoreactivity in the adult human olfactory bulb. HuD (E-1) antibody shows no labeling of microglia (A, Iba1) or astrocytes (B, GFAP), but co-labels many Sox10 expressing cells in the human olfactory bulb (C). A subset of Sox10 expressing cells in the glomerular layer did not show any HuD immunoreactivity (D). Scale bars indicate 20 μ m.

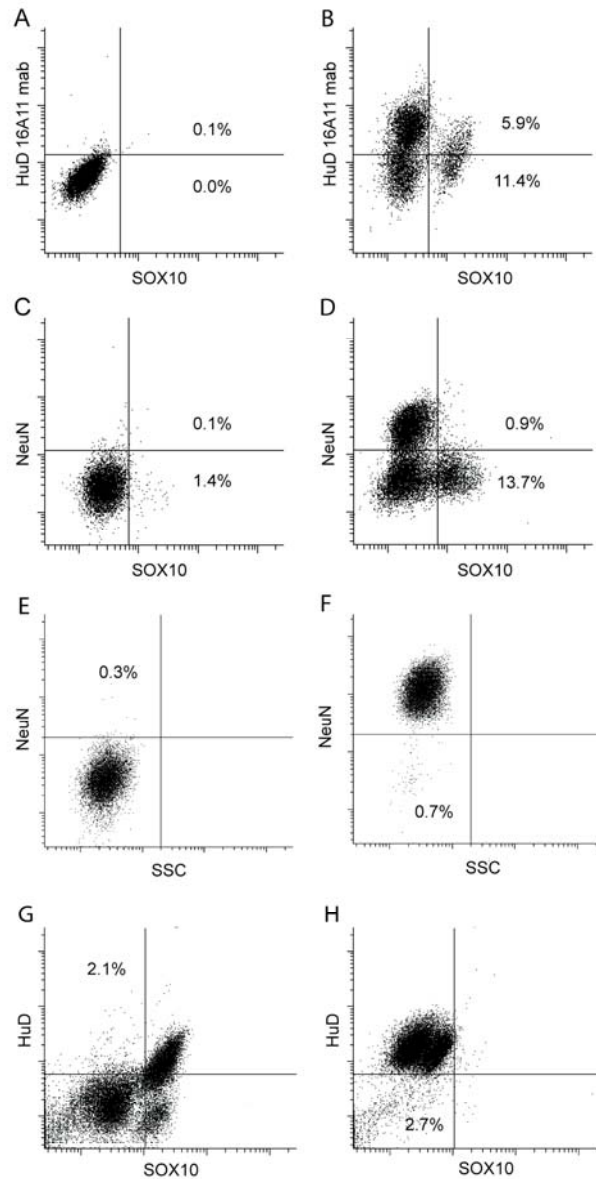


Figure S3, related to Figure 2.

HuD 16A11, but not antibodies to NeuN, labels a subset of Sox10 immunoreactive nuclei in the human olfactory bulb and re-analysis of sorted neuronal and non-neuronal nuclei. (A and B) Co-staining with the neuron specific antibody HuD clone 16A11 (Barami et al., 1995) and Sox10 revealed a partial overlap of populations. Approximately one third of the oligodendrocyte lineage nuclei identified by Sox10 were immunoreactive to the HuD 16A11 antibody, but none were immunoreactive to NeuN (C and D). A and C show labeling with isotype control antibodies. After flow cytometry-based neuronal nuclei isolation the neuronal as well as the non-neuronal populations were re-analyzed for sorting purity. A minimum of 5,000 nuclei were re-analyzed. (E) Contaminating NeuN+ and (F) NeuN- nuclei as well as HuD+/Sox10- (G) and non-neuronal nuclei (HuD- and/or HuD+/Sox10+) (H) can be clearly distinguished. SSC = side scatter.

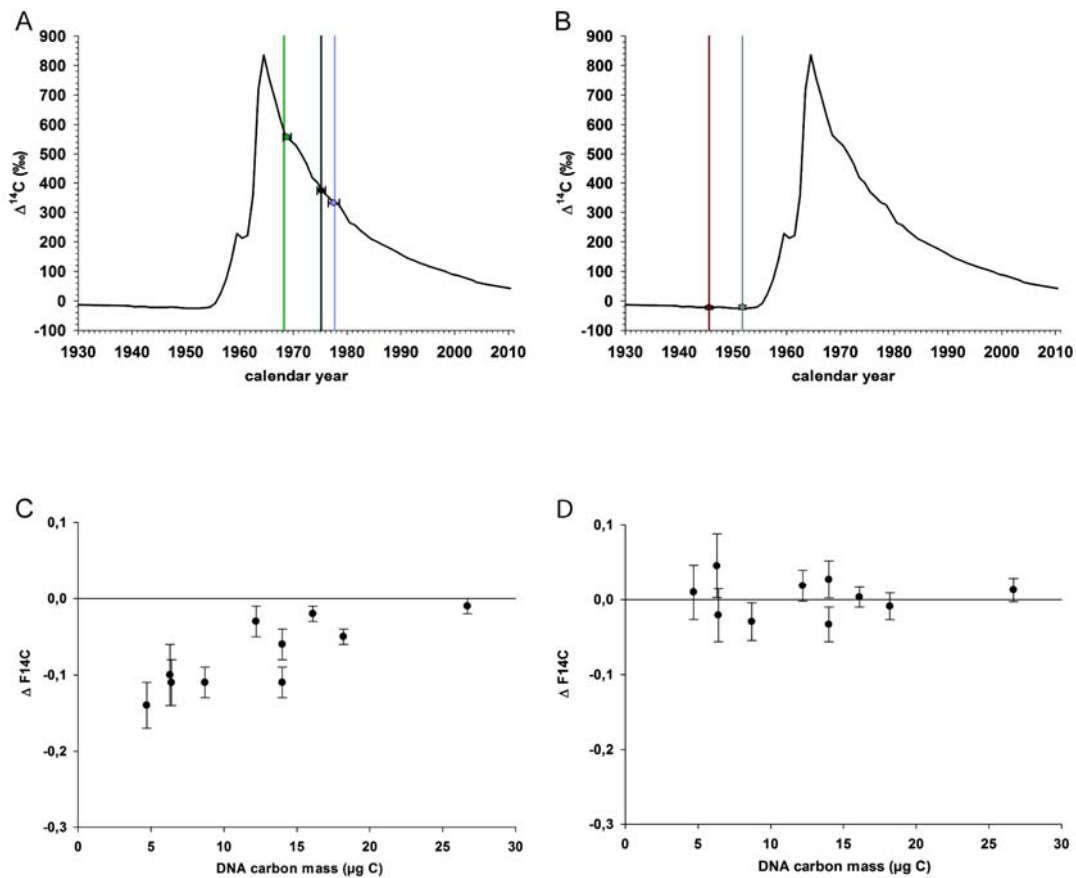


Figure S4, related to Figures 1, 3, and 4.

Carbon background correction strategy for small DNA samples. (A and B) ^{14}C concentrations of cerebellar neurons are not different from the atmospheric ^{14}C value at birth of all the subjects. ^{14}C concentrations of three NeuN-sorted and two non-sorted cerebellar nuclei samples from five different subjects born after ($n = 3$) (A) and (B) before ($n = 2$) the nuclear bomb test indicate no detectable postnatal turnover in the cerebellum. The vertical bars indicate the years of birth, with the correspondingly colored data points indicating the DNA $\Delta^{14}\text{C}$ concentration. Samples exceeding $50\mu\text{g}$ of carbon, measured in the combustion reactor (see Supplemental Experimental Procedures) were selected to establish cerebellar neurons as a no-turnover reference for subsequent AMS analysis of human olfactory bulb samples. (C and D) ^{14}C AMS measurement results for different amounts of DNA from cerebellum neurons of known age. The difference between measured ^{14}C concentrations and nominal ^{14}C concentrations (expected based on the respective birth dates) is depicted for each sample before correction (C) and after correction (D). The average deviation $\Delta\text{F}^{14}\text{C}$ from the nominal value is less than 0.021 ± 0.026 after applying a carbon background correction (see Supplemental Experimental Procedures). Absolute ^{14}C abundances were between $\text{F}^{14}\text{C} = 1.049$ and 1.3835 . Error bars indicate one standard deviation.

Supplemental Experimental Procedures

Correction for FACS impurities

In case the sorting purity was less than 100% (Figures S3E–S3H), we corrected for FACS impurities by solving the following equation system for: $F14C_{Non-Neurons_corrected}$ and $F14C_{Neurons_corrected}$ ($y_{impurity_Non-Neurons}$ and $x_{impurity_Neurons}$ are given in percent). Corrected values are shown in Table S1 (*see accompanying Excel file*).

$$(I) F14C_{Non-Neurons_measured} * 100 = (100 - y_{impurity_Non-Neurons}) * F14C_{Non-Neurons_corrected} + y_{impurity_Non-Neurons} * F14C_{Neurons_corrected}$$

$$(II) F14C_{Neurons_measured} * 100 = (100 - x_{impurity_Neurons}) * F14C_{Neurons_corrected} + x_{impurity_Neurons} * F14C_{Non-Neurons_corrected}$$

Quantitative carbon background correction of ^{14}C AMS results of microgram-size DNA samples

Carbon background incorporated into microgram graphite AMS targets limits the overall ^{14}C measurement precision and thus plays an important role in the present study. DNA samples obtained from human olfactory bulb neurons were of 4-12 μg C size. The respective graphite sputter targets had a carbon mass of 2.3-5.5 μg . Effort was put into understanding carbon background issues quantitatively at all stages of sample preparation (i.e. tissue sampling, cell nuclei extraction, flow cytometry, DNA extraction, DNA sample shipping and handling, freeze-drying, combustion, graphitization and AMS measurement). Part of the DNA specific carbon background investigations are published by Liebl et al. (Liebl et al., 2010). Quantitative background correction of the AMS measurement results was carried out based on AMS results of 15 DNA samples of known ^{14}C concentration, extracted from human cerebellum neurons which underwent the same sample preparation procedures as the DNA samples from human olfactory bulb neurons. Thus, carbon background incorporated at all stages of sample preparation is accounted for. Although the cerebellum has been seen as a late developing organ, most neurogenesis in cerebellum takes place during the gestation period with some proliferation within the first postnatal year (Abraham et al., 2001; Rakic and Sidman, 1970) which was also demonstrated by ^{14}C measurements of larger amounts of DNA (>50 μg C, more robust against carbon background) from the human cerebellum. Genomic ^{14}C concentrations of those large cerebellum samples did not show any significant deviation from atmospheric ^{14}C values at birth in all subjects (Figures S4A and S4B). This allows calculating

nominal ^{14}C concentrations for these samples based on measured ^{14}C concentrations of atmospheric CO_2 from the last 60 years (Levin et al., 2008; Levin and Kromer, 2004; Levin et al., 2010; Reimer et al., 2004). AMS measurement results of DNA samples of cerebellum neurons were fitted to these nominal concentrations by variation of a parametric carbon background model. The 6 background parameters involved in weighted least square fitting (James and Roos, 1975) were a constant amount of 'dead' ($F^{14}\text{C} = 0.00$) and 'modern' ($F^{14}\text{C} = 1.00$) carbon background, which may be added on one hand to the aqueous DNA solution (d_{DNA_dead} and d_{DNA_modern}), but also to the sample CO_2 (m_{CO_2}) in the graphitization reactor ($d_{\text{CO}_2_dead}$ and $d_{\text{CO}_2_modern}$). Furthermore a carbon background of the DNA solution proportional to the DNA mass (m_{DNA}) was assumed.

This background was mathematically split into one 'dead' and one 'bomb' ($F^{14}\text{C} = 2$, slightly above the maximal $^{14}\text{C}/^{12}\text{C}$ ratio in tropospheric CO_2 during the bomb peak era) contribution to allow for residual contamination with proteins with $F^{14}\text{C} \geq 1$ (k_{DNA_dead} and k_{DNA_bomb}).

The background correction

$$F^{14}\text{C}(\text{CO}_2) = \frac{F^{14}\text{C}(\text{AMS}) \times (m_{\text{CO}_2} + d_{\text{CO}_2_dead} + d_{\text{CO}_2_modern}) - d_{\text{CO}_2_modern}}{m_{\text{CO}_2}}$$

was calculated as:

$$F^{14}\text{C}(\text{DNA}) = \frac{F^{14}\text{C}(\text{CO}_2) \times [m_{DNA} \times (1 + k_{DNA_dead} + k_{DNA_bomb}) + d_{DNA_dead} + d_{DNA_modern}] - d_{DNA_modern} - 2 \times m_{DNA} \times k_{DNA_bomb}}{m_{DNA}}$$

$F^{14}\text{C}(\text{AMS})$ denotes the AMS measurement result, $F^{14}\text{C}(\text{CO}_2)$ the $^{14}\text{C}/^{12}\text{C}$ ratio of the sample CO_2 (without the background) and $F^{14}\text{C}(\text{DNA})$ the $^{14}\text{C}/^{12}\text{C}$ ratio of the DNA. The AMS measurement results of DNA samples of human olfactory bulb neurons and cerebellum control samples (Figures S4C and S4D) were corrected for carbon background according to the quantitatively determined background parameters, their uncertainties and correlations. In a first step a correction for a constant dead carbon background of (0.19 ± 0.03) μg incorporated into the CO_2 inside the graphitization reactors was carried out. The CO_2 mass (m_{CO_2}) was determined manometrically as described in Liebl et al. (Liebl et al., 2010). In a second step, a correction of a DNA carbon mass proportional contribution of (8.8 ± 4.4) % with a ^{14}C content of $F^{14}\text{C} = 1.07 \pm 0.13$ was applied. The DNA mass (m_{DNA}) in the aqueous solution, which was shipped for AMS sample preparation was determined by UV spectrometry.

Quality control of sample preparation and AMS measurement methods

Due to the importance of an accurate carbon background correction of ^{14}C AMS results obtained from microgram-size graphite targets we applied several procedures to monitor the carbon background incorporated into our samples along with processing of samples from the human olfactory bulb. Each batch of olfactory bulb samples included the following type of quality control samples: pure water samples, DNA samples split from a DNA master solution and DNA samples from neurons of the cerebellum from the same individuals of which olfactory bulb samples were processed. Carbon quantitation of pure water samples allowed monitoring background incorporated at incubation of DNA samples, shipping and handling, freeze-drying and combustion. Typical amounts of carbon obtained as CO_2 from 0.5 ml pure water were $(0.08 \pm 0.06) \mu\text{g C}$. DNA samples split from a larger amount of DNA allowed to monitor the AMS sample preparation and measurement methods (i.e. shipping and handling, freeze-drying, combustion, graphitization and AMS measurement). The results obtained from these samples were compared with the result of a ^{14}C measurement carried out beforehand on one large sample from the same DNA solution. DNA samples from cerebellum neurons from the same individuals of which olfactory bulb samples were taken were processed and evaluated in the same way as olfactory bulb samples. Thus, the agreement of their result with ^{14}C concentrations of atmospheric CO_2 from the respective birth dates confirms that sample preparation and measurement methods involved at all stages of sample processing are free of irregularities. All three quality control measures confirmed stable background conditions throughout the whole time period in which DNA samples from the human olfactory bulb were processed.

Modeling cell turnover in the human olfactory bulb

The data set contains ^{14}C levels of 15 neuronal DNA samples, 11 non-neuronal DNA samples, and 11 unsorted samples, for a total of 37 data points. Purity-corrected ^{14}C abundances were used when available (see Table S1). We used a cell renewal model in which cells are replaced randomly at a constant rate (Bernard et al., 2010). More detailed models are possible, but the constant turnover rate model is well suited to detect the presence of cell turnover.

We first calculated the global constant turnover rate for each type of sample, neurons, non-neurons, and unsorted samples (Table S3).

Table S3. Summary of the turnover rates for olfactory bulb cell sorts.

	Estimate (per year)	Std error	P-value (=0)
Neurons (n=15)	8.2e-5	0.00075	0.91
Non-neurons (n=11)	0.020	0.0036	0.0002 ***
Unsorted (n=11)	0.0034	0.0012	0.02 *

At first glance, neurons seem to have a very low renewal rate. With 0.0082% per year, after 100 years, less than 1% would be replaced. The confidence interval on the turnover rate estimate includes 0 (95% confidence interval: [-0.0014, 0.0018] per year), and the hypothesis that the turnover is different from zero can be rejected with a p-value = 0.91.

Non-neurons seem to have a positive renewal rate, at around 2% per year as a first estimate, and it is significantly different from zero (p-value = 0.0002). The global fit is not very good, and indicates that there might be changes in turnover rates with aging, or that the non-neuronal sample is heterogeneous, with cells turning over at different rates.

Unsorted samples, which include neurons and non-neuronal cells, showed more renewal than neurons, but less than non-neurons, as expected. The turnover rate was still significantly greater than 0 (p-value = 0.02).

Second, we looked at **individual turnover rates**, calculated for each data point (Table S4).

Table S4. Individual turnover rates for each cell sorts.

	Mean turnover rate	Median turnover rate	T-test (true mean = 0)
Neurons (n=15)	-0.0024	0.00013	0.18
Non-neurons (n=11)	0.035	0.021	0.026 *
Unsorted (n=11)	0.0052	0.0037	0.0078 **

The conclusions are the same as with the global fit: neurons have negligible turnover. Non-neuronal samples showed a negative correlation between turnover rates and age of the subject ($r = -0.69$, p -value = 0.01). We compared homogeneous population scenarios (A: constant turnover; B: constant death and birth rates; C1, C2, C4: decreasing turnover rates with subject age; E2: cumulative cell survival, F1: cumulative damage, birth rate constant, for more information, see the Supplemental online material (Bergmann et al., 2009) and two-population scenarios (no turnover/A, no turnover/B, no turnover/C4). Two-population scenarios were significantly better, with little difference between them (Scenario 2POPB did not give meaningful results). We conclude that a scenario where a significant fraction (64%) of the non-neuronal cells turn over at a rate of around 5% per year explain best the data (Figure S5).

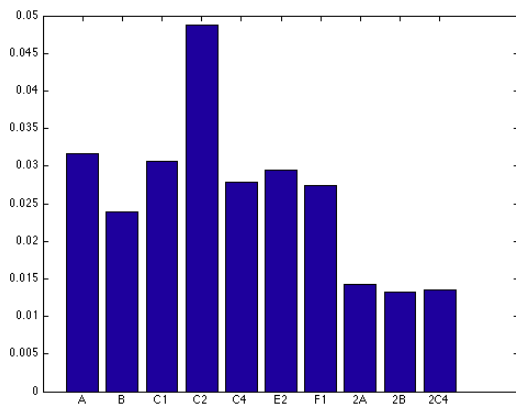


Figure S5. SSE for non-neuron cell turnover scenarios. Lower values for 2A, 2B, 2C indicate heterogeneous turnover rates within the non-neuronal cells.

Bootstrap is a computational method that allows the numerical computation of any kind of statistics [Efron, B., Tibshirani, R., Bootstrap methods for standard errors, confidence intervals, and other measures of statistical accuracy (1985), Statistical science 1:54-77]. It is particularly useful to compute the distribution of an unknown parameter (histogram) when there is only a limited number of samples. The bootstrap approach used here is to perform a least-square fit of the data to a model, and extract the residuals (the difference between the observations and the prediction), and generate a new data set by randomly reassigning the residuals. The model is $Y_i = C(X_i, r) + \varepsilon_i$, where X_i is the date of birth of the i th subject from which the sample was extracted, Y_i is the ^{14}C abundance in the sample, and ε_i is the residual (error) between the prediction of the model ($C(X_i, r)$) and the actual measured value Y_i . The parameter r is the turnover rate of the neuronal population that minimizes the sum of the squares of the residuals, $\sum \varepsilon_i^2$. The values Y_i are thus composed of a deterministic part (the model) and a random (or uncontrolled) part (the residual) that the model does not account for. The residuals include experimental measurement error and physiological effects that were not considered in the model. The effect of measurement error on turnover rate was considered below (no significant turnover was found). Different data set would yield a different value of the turnover rate r . To compute the distribution of possible values of r , we generate a bootstrap replicate of the samples Y_i by randomly reassigning the residuals to each prediction: $\hat{Y}_i = C(X_i, r) + \varepsilon_j$, where j is randomly picked from 1 to n , for each data point (with replacement).

This way, it is possible to artificially inflate the number of observations, while preserving the properties of the original data set, by generating new data sets. We generated $n=999$ bootstrap replicates \hat{Y} , and for each replicate, we calculated the best value of the turnover rate in the least-square sense. This resulted in a distribution of 1000 values of the turnover rate r .

The results show a bias towards higher values of the turnover rate: the mean turnover rate with the bootstraps is 0.00095 per year (0.095% per year), compared to the original estimate of $8.2\text{e-}5$ per year. At the rate of 0.095% per year, it would take more than 700 years to replace half the neurons. The standard deviation is 0.0006 years, which is relatively narrow. Overall the distribution looks like a normal distribution, with almost no outliers. The maximal value is 0.0037 per year and the minimal value is -0.00087 per year. Negative turnover rates for some

bootstrap replicates indicate that neurons would have been formed before birth to account for the ^{14}C abundance observed. Slightly less than 6% of the bootstrap replicates had negative turnover estimates.

Compared to the original turnover rate of $8.2\text{e-}5$ per year, the mean turnover rate of bootstrap replicates is much larger in relative terms. This is due to an artifact of the bootstrap method caused by the difference in interpretation of the ^{14}C levels for subjects born before 1963 (prebomb) and after 1963 (postbomb). Prebomb ^{14}C levels higher than the atmospheric background is indicative of turnover, while postbomb ^{14}C levels higher than atmospheric background is indicative of no turnover. When randomized by the bootstrap method, the residuals have a different effect whether they are assigned to a prebomb or a postbomb data point. Assigning a positive postbomb residual (originally indicating no turnover) to a prebomb point increases the estimate of the turnover. Because postbomb residuals are slightly higher than prebomb residuals (not statistically significant), the net effect is to increase the turnover rate. In that sense, the bootstrap provides a “worst case/maximal turnover rate” scenario.

Finally, we used the error on measurement to generate replicates of the data, assuming the ^{14}C abundance was normally around the measured value, with a standard deviation as the measurement error. As in the bootstrap simulations, we generated $n = 999$ artificial datasets, and obtained a turnover rate estimate for each dataset. The artificial dataset turnover rate was $9.3\text{e-}5 \pm 0.0006$ per year, not significantly different from the original estimate of $8.2\text{e-}5$ per year (one-sample t-test, $p\text{-value} > 0.5$) (Figure S6).

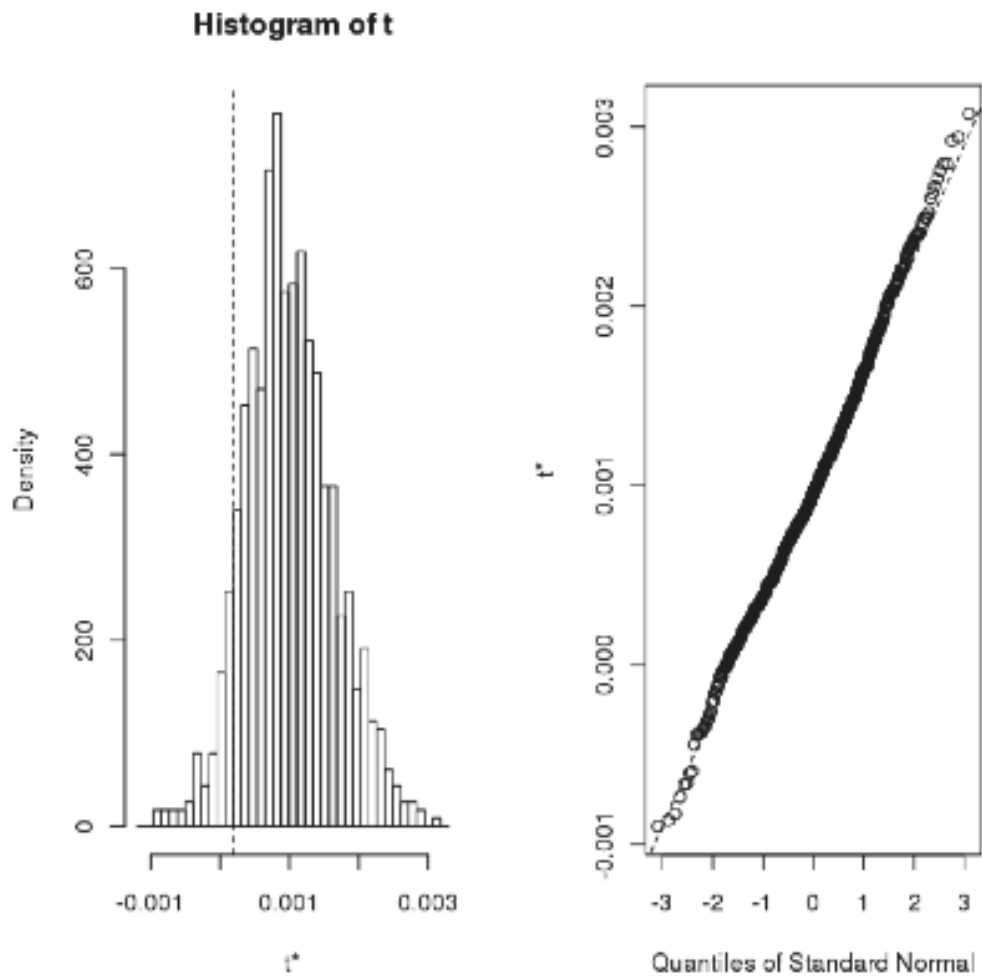


Figure S6. Bootstrap statistics.

The left panel shows the distribution of turnover estimates (the dashed line shows the original estimate). The right panel is a Q-Q plot representing how close the distribution is from a Gaussian distribution.

Supplemental References

- Abraham, H., Tornoczky, T., Kosztolanyi, G., and Seress, L. (2001). Cell formation in the cortical layers of the developing human cerebellum. *Int J Dev Neurosci* 19, 53-62.
- Barami, K., Iversen, K., Furneaux, H., and Goldman, S.A. (1995). Hu protein as an early marker of neuronal phenotypic differentiation by subependymal zone cells of the adult songbird forebrain. *J Neurobiol* 28, 82-101.
- Bergmann, O., Bhardwaj, R., Bernard, S., Zdunek, S., Barnabe-Heider, F., Walsh, S., Zupicich, J., Alkass, K., Buchholz, B., Druid, H., *et al.* (2009). Evidence for Cardiomyocyte Renewal in Humans. *Science* 324, 98-102.
- Bernard, S., Frisén, J., and Spalding, K.L. (2010). A mathematical model for the interpretation of nuclear bomb test derived ^{14}C incorporation in biological systems. *Nuclear Instruments and Methods in Physics Research Section B: Beam Interactions with Materials and Atoms* 268, 1295-1298.
- James, F., and Roos, M. (1975). MINUIT - A system for function minimization and analysis of the parameter errors and correlations. *Computer Physics Communications* 10, 343-367.
- Levin, I., Hammer, S., Kromer, B., and Meinhardt, F. (2008). Radiocarbon observations in atmospheric CO_2 : Determining fossil fuel CO_2 over Europe using Jungfraujoch observations as background. *Science of the Total Environment* 391, 211-216.
- Levin, I., and Kromer, B. (2004). The tropospheric $^{14}\text{CO}_2$ level in mid-latitudes of the northern hemisphere (1959 – 2003). *Radiocarbon* 46, 1261-1272.
- Levin, I., Naegler, T., Kromer, B., Diehl, M., Francey, R.J., Gomez-Pelaez, A.J., Steele, L.P., Wagenbach, D., Weller, R., and Worthy, D.E. (2010). Observations and modelling of the global distribution and long-term trend of atmospheric $^{14}\text{CO}_2$. *Tellus* 63b, 26-46.
- Liebl, J., Avalos Ortiz, R., Golser, R., Handle, F., Kutschera, W., Steier, P., and Wild, E.M. (2010). Studies on the preparation of small ^{14}C samples with an RGA and ^{13}C enriched material. *Radiocarbon* 52, 1394-1404.
- Rakic, P., and Sidman, R.L. (1970). Histogenesis of cortical layers in human cerebellum, particularly the lamina dissecans. *The Journal of comparative neurology* 139, 473-500.
- Reimer, P.J., Brown, T.A., and Reimer, R.W. (2004). Discussion: reporting and calibration of post-bomb ^{14}C data. *Radiocarbon* 46, 1299.
- Uhlen, M., Bjorling, E., Agaton, C., Szgyarto, C.A., Amini, B., Andersen, E., Andersson, A.C., Angelidou, P., Asplund, A., Asplund, C., *et al.* (2005). A human protein atlas for normal and cancer tissues based on antibody proteomics. *Mol Cell Proteomics* 4, 1920-1932.

case ID	KI sample ID	F ¹⁴ C background corrected result	σ(F ¹⁴ C background corrected result)	F ¹⁴ C FACS purity corrected result	year of measurement	delta ¹⁴ C (‰)	delta ¹⁴ C (‰) purity corrected	Formation Year	date of birth	tissue	immunolab
6	O487	1.4260	0.0627	NA	2011	415.5161	NA	1974.33	1976.8	olfactory bulb	Hud+/Sox
7	O489	1.4728	0.0383	1.4832	2011	461.9721	472.2604	1971.67	1974.3	olfactory bulb	Hud+/Sox
11	O483	0.9881	0.0189	0.9862	2011	-19.1644	-21.0693	NA	1955.7	olfactory bulb	Hud+/Sox
15	O491	1.1848	0.0298	1.1889	2011	176.0894	180.1871	1987.84	1990.5	olfactory bulb	Hud+/Sox
19	O473	1.0038	0.0245	1.0019	2011	-3.5799	-5.4444	NA	1946.0	olfactory bulb	Hud+/Sox
22	O468	0.9957	0.0307	0.9892	2011	-11.6203	-18.0833	NA	1938.0	olfactory bulb	Hud+/Sox
2	O423	1.0055	0.0350	NA	2011	-1.8924	NA	NA	1954.1	olfactory bulb	Hud+/Sox
7	O490	1.2230	0.0433	1.2198	2011	214.0086	210.8719	1984.38	1974.3	olfactory bulb	HuD- and/or ̵
11	O484	1.1004	0.0121	1.1019	2011	92.3099	93.8032	NA	1955.7	olfactory bulb	HuD- and/or ̵
15	O492	1.0724	0.0303	1.0715	2011	64.5158	63.6471	2003.50	1990.5	olfactory bulb	HuD- and/or ̵
19	O474	1.1334	0.0163	1.1361	2011	125.0673	127.7308	NA	1946.0	olfactory bulb	HuD- and/or ̵
22	O469	1.1308	0.0151	1.1372	2011	122.4864	128.8025	NA	1938.0	olfactory bulb	HuD- and/or ̵

case ID	KI sample ID	F ¹⁴ C background corrected result	σ(F ¹⁴ C background corrected result)	year of measurement	delta ¹⁴ C (‰)	Formation Year	date of birth	tissue	immunolab		
5	O486	1.0140	0.0337	NA	2011	6.5451	NA	NA	1940.3	olfactory bulb	non-sorte
23	O482	1.4910	0.0193	NA	2011	480.0383	NA	1971.57	1970.1	olfactory bulb	non-sorte
14	O280	1.0712	0.0208	NA	2010	63.4532	NA	NA	1946.9	olfactory bulb	non-sorte
18	O163	1.0235	0.0250	NA	2010	16.0982	NA	NA	1956.5	olfactory bulb	non-sorte
16	O282	1.4957	0.0269	NA	2010	484.8833	NA	1971.07	1971.5	olfactory bulb	non-sorte
30	O372	1.3485	0.0197	NA	2011	338.5859	NA	1977.00	1973.8	olfactory bulb	non-sorte
28	O331	1.2380	0.0108	NA	2011	228.8983	NA	1982.69	1979.5	olfactory bulb	non-sorte
29	O333	1.2262	0.0139	NA	2011	217.1851	NA	1983.70	1980.6	olfactory bulb	non-sorte
20	O427	1.0695	0.0223	NA	2011	61.6371	NA	NA	1933.6	olfactory bulb	non-sorte
4	O435	1.0271	0.0580	NA	2011	19.5488	NA	NA	1948.2	olfactory bulb	non-sorte
21	O444	0.9630	0.0239	NA	2011	-44.0799	NA	NA	1955.8	olfactory bulb	non-sorte

case ID	KI sample ID	F ¹⁴ C background corrected result	σ(F ¹⁴ C background corrected result)	F ¹⁴ C FACS purity corrected result	year of measurement	delta ¹⁴ C (‰)	delta ¹⁴ C (‰) purity corrected	Formation Year	date of birth	tissue	immunolab
13	O279	0.9921	0.0155	NA	2011	-15.1939	NA	NA	1945.6	olfactory bulb	NeuN+
9	O275	0.9796	0.0436	NA	2011	-27.6020	NA	NA	1948.1	olfactory bulb	NeuN+
24	O314	0.9861	0.0299	NA	2011	-21.1497	NA	NA	1952.3	olfactory bulb	NeuN+
27	O358	1.366	0.0342	NA	2011	355.9573	NA	1976.30	1977.7	olfactory bulb	NeuN+
1	O174	1.2995	0.0153	NA	2010	290.1022	NA	1979.30	1977.7	olfactory bulb	NeuN+
17	O284	1.2457	0.0168	1.2467	2011	236.5417	237.5441	1982.22	1983.8	olfactory bulb	NeuN+
8	O317	1.0076	0.0208	NA	2011	0.1922	NA	NA	1950.6	olfactory bulb	NeuN+
3	O511	0.9649	0.0181	NA	2011	-42.1939	NA	NA	1946.8	olfactory bulb	Fox3+
25	O311	1.0578	0.0249	NA	2011	50.0231	NA	NA	1950.0	olfactory bulb	NeuN-
8	O260	1.0206	0.0352	NA	2011	13.0966	NA	NA	1950.6	olfactory bulb	NeuN-
12	O277	1.4052	0.0178	NA	2011	394.8691	NA	1974.40	1966.0	olfactory bulb	NeuN-
26	O313	1.3185	0.0177	NA	2011	308.8065	NA	1978.31	1969.0	olfactory bulb	NeuN-
10	O276	1.1580	0.0180	NA	2011	149.4865	NA	1990.41	1981.3	olfactory bulb	NeuN-
17	O285	1.1354	0.0235	1.1345	2011	127.0526	126.1615	1992.99	1983.8	olfactory bulb	NeuN-

Legends

NA not applicable/not available

SUPPLEMENTAL TABLE 1

case ID	age	YoB	YoD	sex	manner of death	cause of death	psychiatric history	drug abuse
1	29	1977	2007	M	drug intoxication	accident	poly drug use	YES
2	53	1954	2007	F	traumatic chest injuries	undetermined	MDE, alcohol intoxication	YES
3	61	1946	2008	F	drug intoxication	undetermined	RDD, Mixed anxiety and depressive disorder	NO
4	59	1948	2008	M	hanging	suicide	anxiety disorder	NO
5	69	1940	2009	M	acute myocardial infarction	natural	NO	NO
6	32	1976	2009	M	hanging	suicide	psychotic disorder due to poly drug use	YES
7	35	1974	2009	M	hanging	suicide	no diagnosis, visited psychiatric outpatient service in 2008	NO
8	59	1950	2009	M	Ischemic heart disease	natural	alcohol dependence	YES
9	61	1948	2009	M	acute myocardial infarction	natural	NO	NO
10	28	1981	2009	M	traumatic chest injuries	suicide	RDD	NO
11	54	1955	2009	M	alcohol intoxication	undetermined	no data	no data
12	43	1965	2009	F	myocarditis	natural	RDD	NO
13	64	1945	2010	M	multiple traumatic injuries	accident	NO	NO
14	63	1946	2010	F	suffocation	suicide	RDD	NO
15	19	1990	2010	M	hanging	suicide	o psychiatric dignosis, visited child&adolescent health service in 200	NO
16	39	1971	2010	F	drug intoxication	suicide	MDE, poly drug use	YES
17	27	1983	2010	M	traumatic chest injuries	accident	ADHD, poly drug use	YES
18	54	1956	2010	M	cardiomyopathy	natural	MDE, alcohol dependence	YES
19	64	1946	2011	M	diabetic coma	natural	RDD	NO
20	77	1933	2011	M	Ischemic heart disease	natural	no data	no data
21	55	1955	2011	M	ruptured aortic aneurysm	natural	alcohol dependence	YES
22	73	1938	2011	M	drug intoxication	undetermined	RDD	NO
23	41	1970	2011	M	hanging	suicide	RDD, anxiety disorder	NO
24	53	1952	2005	F	blood loss from periferal vessels	suicide	RDD, poly drug use	NO
25	57	1949	2006	M	acute myocardial infarction	natural	NO	NO
26	37	1968	2006	M	traumatic chest injuries	suicide	paranoid episodes, asperger syndrom	NO
27	36	1977	2007	M	drug intoxication	undetermined	RDD, panic disorder	NO
28	29	1979	2008	M	drug intoxication	suicide	MDE	NO
29	28	1980	2008	M	hanging	suicide	MDE	NO
30	35	1973	2008	M	choking	accident	NO	NO

Abbreviations

MDE Major depressive episode
RDD Recurrent depressive disorder
ADHD Attention deficit hyperactivity disorder
YoB Year of Birth
YoD Year of Death

SUPPLEMENTAL TABLE 2